3D SIMULATION OF GAS FLOW IN A CYCLONE USING A COMMERCIAL CFD CODE

Bernardo, S.
Department of Chemical Processes, School of Chemical Engineering, State University of Campinas, C.P. 6066, CEP 13083-970, Campinas, SP, Brazil
bernardo@feq.unicamp.br

Mori, M.
Department of Chemical Processes, School of Chemical Engineering, State University of Campinas, C.P. 6066, CEP 13083-970, Campinas, SP, Brazil
mori@feq.unicamp.br

Abstract. This work presents information about pressure and velocities profiles inside cyclones and analyse of the influence of geometry, grid and initial gas velocity in flow system. A set of governing partial differential equations consisting of mass and momentum conservation equations was solved by FLUENT version 6.0, a commercial Computational Fluid Dynamics (CFD) code available on market. The grids were constructed by multi-block technique using ICEM CFD HEXA and Gambit softwares. Two turbulence models were used in this work: standard k-ε and Re-Normalization Group k-ε (RNG k-ε) turbulence model, with higher upwind interpolation scheme and SIMPLEC method to pressure-velocity coupling algorithms. Results showed that ICEM CFD HEXA generated grids less refined than Gambit software, but this one required less computational effort and supplied best numerical results. About gas flow, results showed a gas symmetrical tangential velocity profile and swirl regions existing inside cyclone. A good agreement was achieved with experimental data.

Keywords: CFD, Cyclones, Gas Flow, FLUENT, turbulence.

1. Introduction

Gas cyclone separators are widely used in industrial processes to separate dust from gas streams or product recovery. They are normally tangential entrance inlets in design and are defined as funnel-shaped industrial inertial devices. Its popularity is due to the fact that it is simple and inexpensive to manufacture, compact, contains no moving parts and requires very little maintenance. It's chief disadvantage is its rather pressure drop (and power requirement) as compared to simple settling chambers (Boysan et al., 1982).

An important application of cyclones is the recovery of catalyst in fluid catalytic cracking (FCC) units. The gas cyclone in FCC is generally used in a multi-cell arrangement to meet recovery requirements of typically more than 99%. At a further stage, a high-efficiency cyclone system may be used to remove the remaining particles. The gas cyclone used at this stage operates at low solids loading, with the particles having a diameter in the range of 0.1-80 μm. High collection efficiencies (more than 99.9%) are demanded, e.g., to meet environmental regulations on dust emission and/or to prevent excessive wear of turbine blades in energy/recovery systems (Hoekstra et al.,1999).

The design of the cyclone, in its common form, has survived largely unchanged for over a century. In general, cyclone designs fall into two groups: the straight-through cyclone and the more common conventional or reverse-flow cyclone. Cyclones can be distinguished from others separators by noting that the streamlines complete several revolutions about the axis, the centrifugal forces so produced being the means of separations. Cyclone's operational characteristics are mainly determinated by the density differences of the fluid and particulate phases, and the high rotational velocities and centrifugal forces that are imparted due to the injection of both phases into the upper part of cyclone. As the fluid enters through the inlet (only tangential inlets are considered in the applications described in this paper) near the top of the cyclone, it is constrained to take up a swirling motion. A fraction of this flow, referred to as the under flow, leaves the cyclone through a duct at the base apex of the inverted cone while the rest of reverses direction and swirls upwards to exit from the vortex finder. In addition to the interaction between the particulate and fluid phases, the fluid phase swirls and recirculates inside the cyclone. The flow field inside a cyclone is very complex (Griffiths et al., 1996).

The lack of any really fundamental understanding of the separation process which could lead to such improved performance is due to the fact that despite their apparent simplicity, the cyclones fluid dynamics is complex, including such features as high preservations of vorticity and in some cases several annular zones of reverse flow. The theory of such confined vortex flows has so far been unable to predict many features of the observed flow fields. The problem associated with mathematical modelling of the detailed flow patterns involves the solution of the strongly coupled, non-linear partial differential equations of the conservation of mass and momentum, and lies well beyond any foreseeable analytical approach. In addition, we have found that the turbulence closures based on the assumption of isotropy (e. g. k-ε model) are inapplicable in the case of highly swirling flows (Boysan et al., 1982).

The solution of these equations by numerical techniques have been made possible by advent of powerful digital computers, opening avenues towards the calculation of complicated flow fields with relative ease. The underlying methodology in Computational Fluid Dynamics (CFD) is to subdivide the solution domain into a large number of control volumes and to convert the partial differential equations by integration over these control volumes into their

algebraic equivalents. The result is a set of simultaneous algebraic equations that can be solved using iterative methods to obtain the field distributions of such dependent variables, as velocity components and pressure, subject to the appropriate boundary conditions defining the individual problem.

The exploitation of CFD software for the numerical calculation of the gas flow field is a more generic way of modelling, and may, in principle, yield better predictions on the collection performance of a cyclone (Hoekstra et al., 1999). One of the first CFD calculations of the flow in an industrial cyclone was made by Boysan (1982). An important issue that needs to be addressed for this type of calculations is the effect of turbulence on the gas flow field. Turbulent closure models known in literature for Eulerian frameworks have some weaknesses and modelling uncertainties and their performance still needs to be judged by experimental data.

Earlier experimental studies of flow patterns and collection performance in cyclones were reported by Shepherd and Lapple (1939, 1940), Ter Linden (1949), and Smith (1962). These and others works have been reviewed by Caplan (1977), Ogawa (1984) and Leith (1984).

The aim of this paper is to use the modern techniques in CFD to study the flow of the gas in cyclones through numerical experiments carried through with code FLUENT version 6.0. FLUENT is a general purpose computer program for modelling fluid flow, heat transfer and chemical reaction. It can quickly analyse complex flow problems. This code incorporates up-to-date modelling techniques and wide range of physical models for simulating numerous types of fluid flow problems.

This work is based on two studies of case. The first one of them is of Yuu et al.(1978) and as, of Patterson and Munz (1996), which they supply the experimental data for the validation of the numerical experiments. Also is made a comparative study with the numerical work of Peres et al. (2002), that has worked with another computational code in CFD.

2. Mathematical Modelling

In accordance with Slaterry (1972), the conservation equations of the flow involved phases can be written in a euleriano referential, in its continuous integral or differential form, from the theorem of transport. The conservation equations (continuity equation and the equations of motion) can be written in its generalized form. The time-average mathematical models, together model with the Reynolds decomposition, can be written as follow:
Continuity Equation:

$$\frac{\partial \rho}{\partial t} + \nabla.(\rho u) = 0. \tag{1}$$

Motion Equation:

$$\frac{\partial\, \rho u}{\partial t} + \nabla.(\rho\, u\, u) = \nabla p - \nabla.(\tau + \overline{\rho u' u'}) + \rho g \tag{2}$$

where: **u** is the vector speed, **g** is the gravitational field, **τ** is the strain stress, and $\overline{\rho u' u'}$ is the Reynolds stress. These equations are applicable to incompressible and transient cyclones flow in a 3D coordinates systems.

2.1- Turbulence Modelling

The flow field in a cyclone separator can be considered as a special case of swirling flow, as additional complex flow features, such as axial flow reversal and subcriticality which strongly affect the mean velocity field as well as the turbulence distribution (Hoekstra et al., 1999).

In this work, we work with two turbulence models: the standard k-ε model and the ReNormalization Group (RNG) k-ε model.

The k-ε standard model is a turbulence model in which it assumes the Reynolds stresses are proportional to mean velocity gradients, with the constant of proportionality being characterized by turbulent viscosity μ^t known as Boussinesq eddy-viscosity approach. The k-ε standard model presents two transport differential equations, the first one refers to the turbulent kinetic energy (k) and the second one to dissipation rate of turbulent kinetic energy (ε) as follow:

$$\frac{\partial\, \rho k}{\partial t} + \nabla.(\rho u k) = \nabla.\left[\left(\mu + \frac{\mu^t}{\sigma^k}\right)\nabla k\right] + G - \rho\varepsilon \tag{3}$$

and

$$\frac{\partial\, \rho \varepsilon}{\partial t} + \nabla.(\rho u \varepsilon) = \nabla.\left[\left(\mu + \frac{\mu^t}{\sigma^k}\right)\nabla \varepsilon\right] + \frac{\varepsilon}{k}(C_1 G - C_2 \rho\varepsilon) \tag{4}$$

where G is the generation of turbulence due to velocity gradients:

$$G = \mu^{eff} \nabla u.\left[\nabla u + (\nabla u)^T\right] \tag{5}$$

and the viscosities are represented by:

$$\mu^t = C_\mu \rho \frac{k^2}{\varepsilon}, \quad \mu^{eff} = \mu + \mu^t \tag{6}$$

Here, the empirical constants have the following empirically derived values:

$C_\mu = 0{,}09$; $\sigma^k = 1{,}00$; $\sigma^\varepsilon = 1{,}30$; $C_1 = 1.44$; $C_2 = 1.92$.

In the RNG-k-ε model, the effect of rotation is included in the calculation of the turbulent viscosity. This results in an improved prediction of the shape of the swirling profile for the large vortex finder. The equations for the kinetic energy and its dissipation rate are similar to the standard k-ε model equations, but for the RNG-derived constants assume different values (Here, $C_1 = 1.42$ and $C_2 = 1.68$). The main differences between the RNG-based- k-ε model and the standard one are the calculation of the turbulent viscosity in the case of RNG from the solution of an ordinary differential equation, which includes the effects of rotation and the presence of an additional term in the dissipation rate transport equation (Griffiths et al., 1996).

2.2- Numerical Methods

The simulations in this work were performed by use of the commercial finite volume flow solver FLUENT version 6.0, in which the control volume method is used to discretize the transport equation. The pressure-velocity coupling algorithms used is this work were SIMPLE (Semi IMPlicit Linked Equations) and SIMPLEC (SIMPLE Consistent). About interpolation scheme, we used QUICK and first order upwind and higher upwind. More details about these schemes can be found in Patankar (1980). Numerical experiments were carried out with accuracy of 10^{-6} for the euclidean norm of the source mass in the pressure-velocity coupling.

2.3- Cyclone Geometry and Grid

The geometric properties for a generic cyclone are illustrated in the Fig.(1). In this figure are indicated regions used to form the blocks in the numerical grid and the nomenclature for the equipment geometric specification.

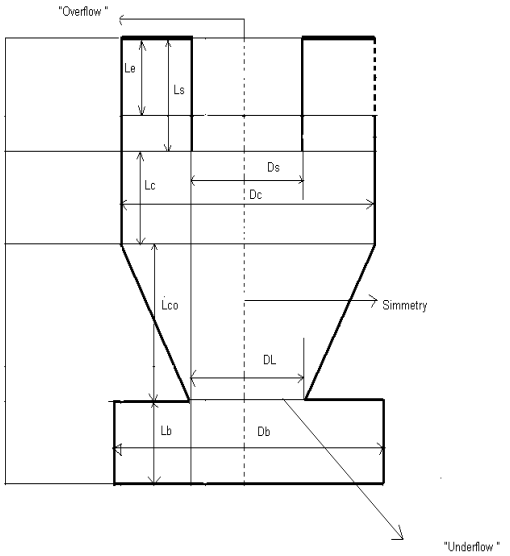

Figure 1: Cyclone Transversal Schematic Representation.

Two types of cyclone that have undergone experimental investigation were studied using CFD techniques. Specifically, these are the cyclones of Yuu et al.(1978) and Patterson et al.(1996). The geometrical features and operational conditions of these cyclones are showed in Table (1). From these data we had constructed the cyclones numerical grids, using for this two mesh building codes: ICEM CFD HEXA and GAMBIT. We have evaluated the influence of the grid refinement, generated from both pre-processors in the simulation process. The final grids that we have used consisted of about 40872 cells (cases 1 e 2) and 42696 cells (case 3). These grids are showed in Fig. (2) and Fig. (3), respectively.

The boundary conditions were considered uniform profiles at the inlet for all variables, no slip conditions at the walls and atmospheric pressure conditions were assumed at the outlet.

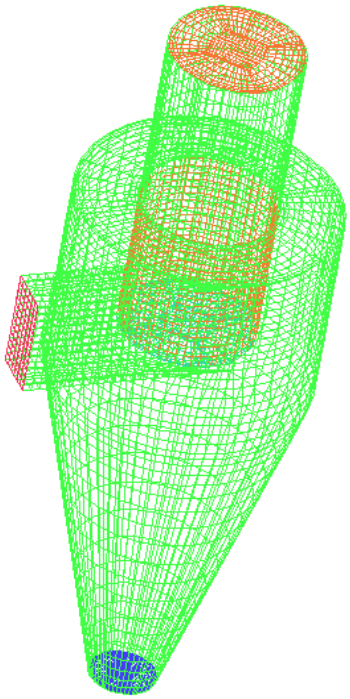

Figure 2: Grid used to cases 1 and 2.

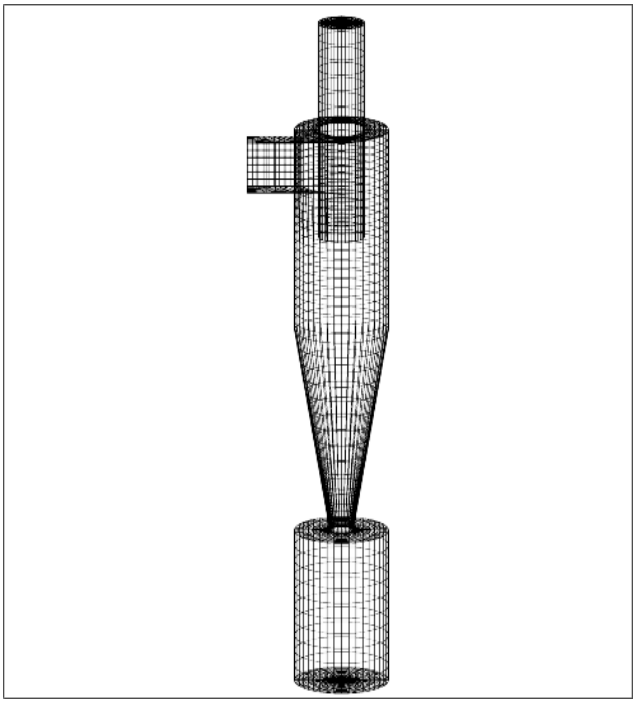

Figure 3: Grid used to case 3

Table 1: Yuu and Patterson cyclones configurations and operating conditions.

PROPERTIES		Case 1: Yuu et al. (1978)	Case 2: Yuu et al. (1978)	Case 3: Patterson et al. (1996)
Operating Conditions	Inlet velocity (m/s)	9,80	13,40	15,20
	Gas flux(m^3/s)	0,05929	0,08107	0,019613
	Fluido	Air	Air	Air
	Temperature (K)	293,15	300	300
	Re_{Dh}	44363,10	58363,10	31776,82
Phisychs Properties	ρ (kg/m^3)	1,142	1,142	1,142
	μ (kg/m.s)	$1{,}85.10^{-5}$	$1{,}85.10^{-5}$	$1{,}85.10^{-5}$
Geometrical Features	a (m)	0,1100	0,1100	0,0508
	h (m)	0,0600	0,0600	0,0950
	H (m)	0,6200	0,6200	0,4060
	b (m)	0,0550	0,0550	0,0254
	Ls (m)	0,1600	0,1600	0,1080
	L_b (m)	-	-	0,1520
	D_C(m)	0,2960	0,2960	0,1020
	D_s(m)	0,1520	0,1520	0,0508

3. Results and Discussion

Table (2) shows a comparison of computational effort for the pre-processors used to generate the grids. The simulations in this test were carried out using cases 1 and 3, working with 2000 steady state iterations.

Table 2: Influence of the grid refinement on computational effort.

Test	Pre-processor	Grid cells number	Computational time (h)
Case 1	Gambit	103013	24 -48
Case 1	ICEM-CFD Hexa	40872	6-12
Case 3	Gambit	303258	48-72
Case 3	ICEM-CFD Hexa	42696	6 -12

We can see that Gambit grid requires more computational effort to achieve convergence. In relation to the grid refinement, we show in Fig.(4) of the tangential velocity profiles for each type of grid 1.

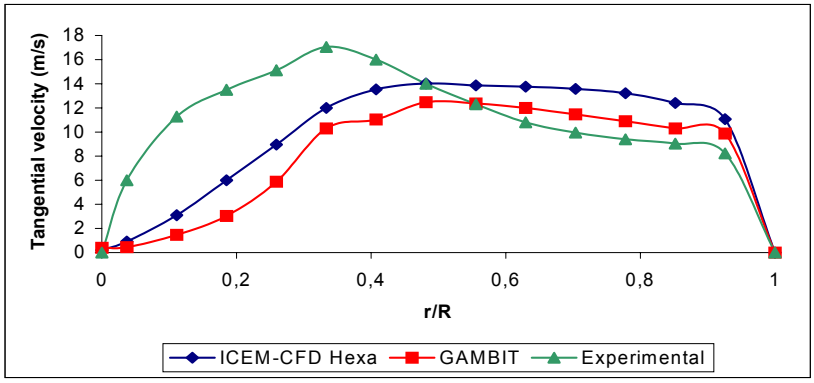

Figure 4: Comparison between tangential velocity profile and pre-processors in case 1.

The same trend of attainment better velocities profiles, using the grids from ICEM-CFD Hexa, was also observed for the case 3. Then, taking into account the computational effort and the tangential velocity profile, we decided to carry out the numerical experiments using grids generated by ICEM-CFD Hexa.

Results from numerical experiments using k-ε standard model showed good stability and the convergence was achieved using steady-state simulation. But the data from these tests were not satisfactory when compare to experimental profile. Fig.(5) shows a map of simulation considering case 1 using k-ε standard model. There, we can verify the observations made before. The profile for all cases using k-ε standard model won´t be presented is this paper.

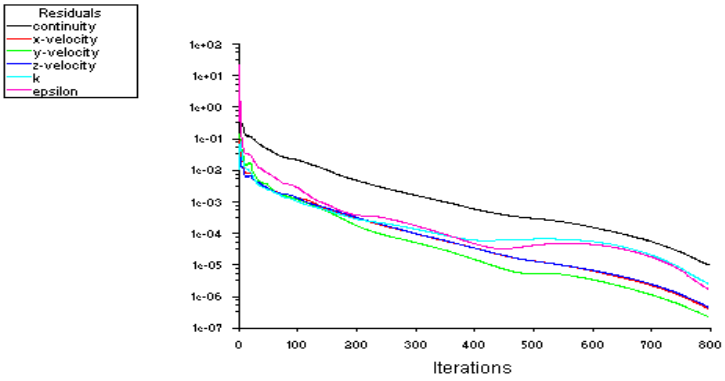

Figure 5: Residual mass in case 1 using k-ε standard model.

Take into account this results, was used another RNG-based-k-ε model viscosity model in the simulations. In this cases, a converged steady-state solution was considered to be one for which characteristic values did not change significantly for at least 1000 time step, according by FLUENT. After this stage, simulations were made in transient state.

3.1. Results for cases 1 and 2:

Cases 1 and 2 refer to the same cyclone geometry. The results for these cases will be presented at the same time. Fig.(6a) and Fig.(6b) show pressure and velocity maps, respectively, in which we can observe a cyclone axial plane. Fig.(6c) shows a comparative between numerical and experimental results for case 1. Fig.(7a) and Fig.(7b) show, respectively, pressure and velocity maps and Fig.(7c) shows a comparative between numerical and experimental results for case 2.

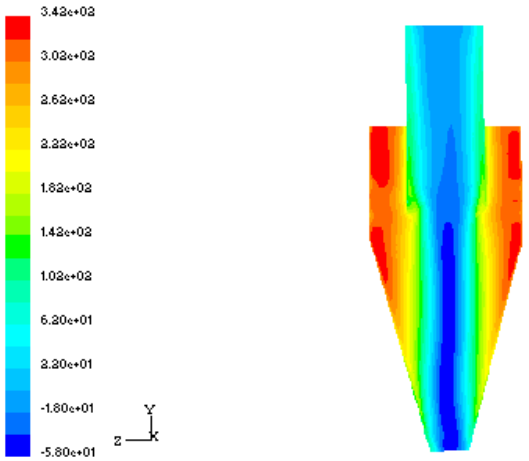

Figure 6a: Pressure field map (case 1).

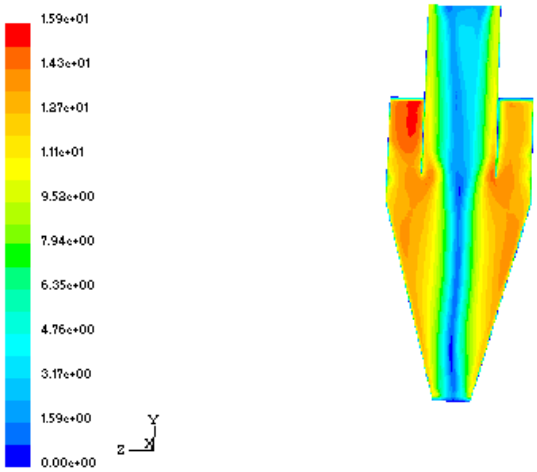

Figure 6b: Velocity field map (case 1)

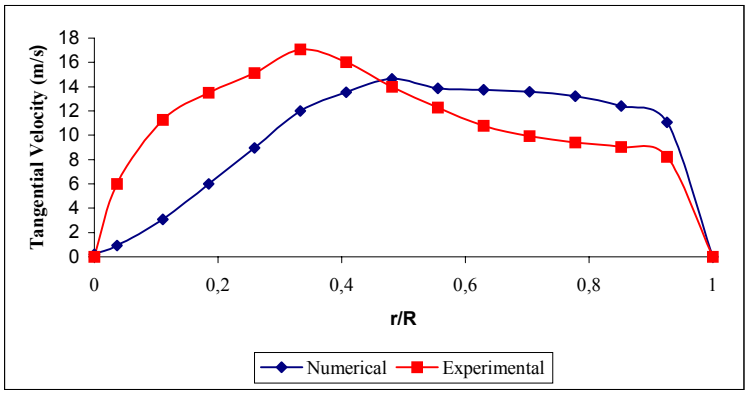

Figure 6c: Tangential velocity profile: Numerical results and Experimental data (case 1).

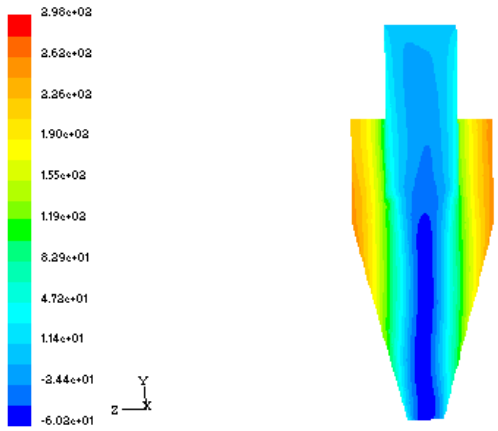

Figure 7a: Pressure field map (case 2).

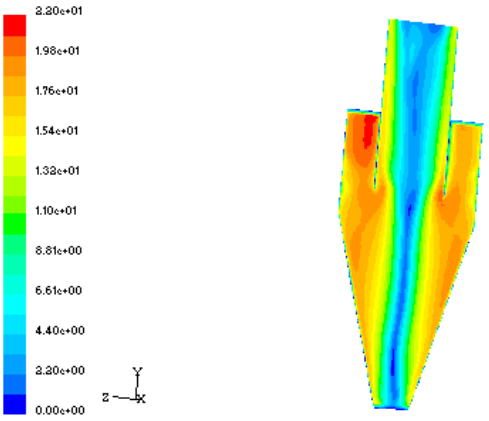

Figure 7b: Velocity field map (case 2).

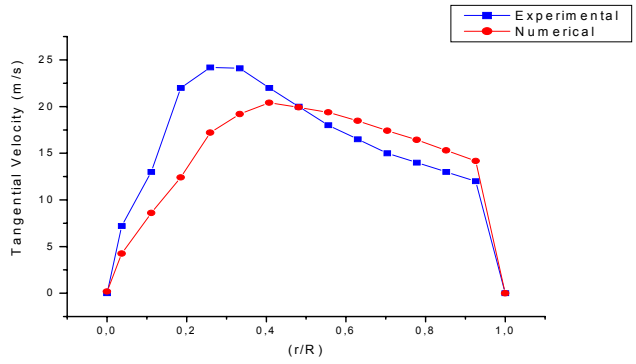

Figure 7c: Tangential velocity profile: Numerical results and Experimental data (case 2).

Fig. (6b) and Fig. (7b) show maximum velocity peaks in red colour located between symmetric axis and the vortex finder (in agreement with Ogawa (1997)). Near the wall, the gas is flowing downwards. When the flow gas expansion occurs in the cylindrical inlet section, it starts the reverse flow (colour changes from red to blue in Fig. (6b) and Fig. (7b)). This gas expansion occurs in all parts of the cyclone. Meier (1998) described that this phenomena, in associated with the high vortex preservation and occurs when the cyclone has insufficient height in the point of view of its natural height (for more details about cyclone natural height concept see Alexander (1949)). The geometric features of the cyclone used in this study are in accordance with before affirmation and this is the reason for the behaviour presented. The velocity symmetrical profile can be check in the Fig. (6b) and Fig. (7b). The tangential velocity profiles (Fig. (6c) and Fig. (7c)) at various axial stations are rather similar. They are in agreement with experimental results.

Fig. (6a) and (7a) show that there is zone of high pressure on cyclone inlet, and this characteristic reduces according the flow downs to conical part. This is also observed in radial position. We can see a low pressure zone situated next to

vortex finder and symmetry axis. It is a very important point on cyclone fluid dynamics since as the pressure zone decreases as low zone of high vortex and faster will be the reverse flow.

Fig. (8) shows a comparison with Peres et al.(2001), where the author made numerical experiments using the same cases with another CFX code. A good agreement was achieved.

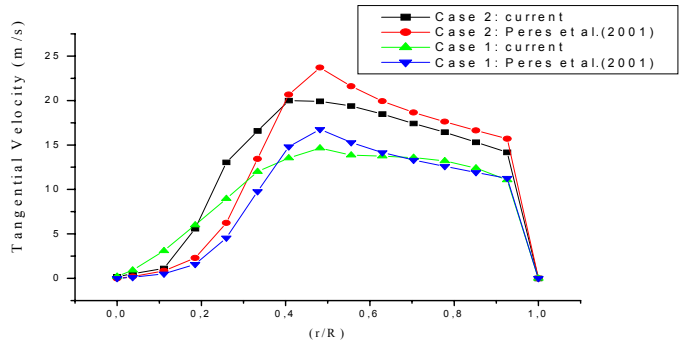

Figure 8: Tangential velocity profiles for numerical experiments involving cases 1 and 2 for current work and Peres et al.(2001).

3.2. Results for case 3:

Fig.(9a) and (9b) show pressure and velocity map, respectively, while Fig.(9c) shows a comparison between numerical and experimental results for case 3.

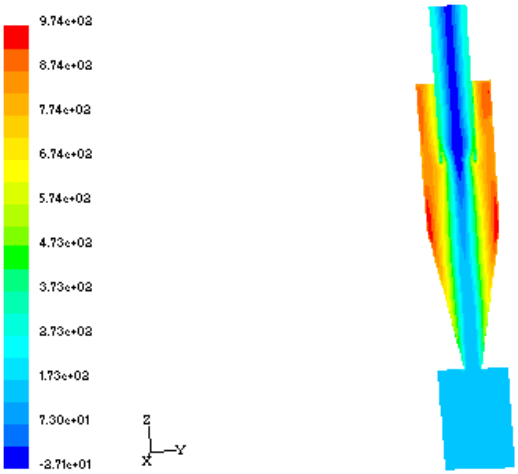

Figure 9a: Pressure field map (case 3).

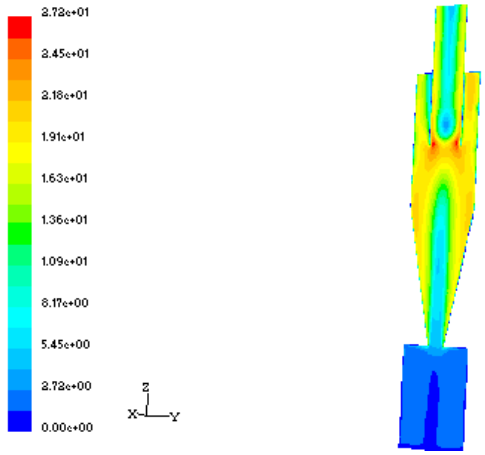

Figure 9b: Velocity field map (case 3).

The cyclone used in this case is smaller than the one used on cases 1and 2. The same behaviour about gas flow (cases 1 and 2) was observed here in the case 3.Maybe we can attribute this fact to cyclone geometric features, agreement with the work of Alexander (1949).

A good agreement with experimental data was achieved, according to Fig. (10) below. A low number of experimental data available on case 3 didn´t allow us to show more details in this validation. But tangential velocity profile presents good agreement in this case.

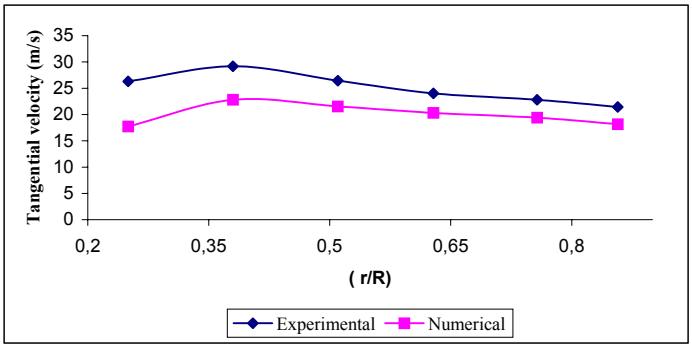

Figure 10: Tangential velocity profile: Numerical results and Experimental data (case 3).

4. Conclusions

In this work, we studied the gas flow in a cyclone using FLUENT. We can see that gas turbulent swirling flow on cyclone separators presents a complex fluid dynamic behavior. The grid refinement for all cases was better using ICEM CFD Hexa as pre-processor. About the turbulence model, was observed that turbulence models based on the assumption of isotropy, like standard k-ε model, is inapplicable for the swirling flow in a cyclone. The RNG-based-k-ε showed very good in this case. All numerical results obtained with FLUENT achieved good agreement with both experimental data and others numerical data and could show some of most complex phenomenon inside cyclone. We verifying that occurs a dislocating of maximum velocity peak on numerical data. This behaviour was also observed by Peres et al.(2001) and requires more numerical experiments to analyse accurately.

5. Acknowledgements

The authors are grateful to FAPESP (process number 00/03966-3) for the financial support in this project.

6. Nomenclature

a – Inlet pipe height, (m);
b – inlet pipe width, (m);
D_C – Cyclone diameter, (m);
D_e- Outlet pipe diameter, (m);
Ds: Diameter of the top exit pipe (“overflow”);
Dc: Cyclone Diameter;
DL: Diameter of the bottom exit pipe (“underflow”);
Db: Hopper diameter;
G- Turbulence generation;
g- Gravity acceleration, (m/s^2);
h- Conical section height, (m);
H- Cyclone height, (m);
k- Turbulent kinetic energy, (m^2/s^2);
Le: Height of the inlet rectangular section;
Ls: Height of the top exit pipe (“overflow”);
Lc: Height of the cylindrical region;
Lco: Height of the conical region;
Lb: Height of the hopper;
Re_{Dh}- Reynolds number (referent to hydraulical diameter);
L_S- Gas outlet pipe length, (m);
t- Time, (s);
u- Velocity vector, (m/s).
ε- Dissipation rate of turbulent kinetic energy, (m^2/s^2);

κ- Bulk viscosity, (kg/ms);
μ- Dynamic viscosity (kg/ms);
ρ- Density, (kg/m^3);
σ- k-ε model constant;
τ- Viscosity stress, (M/LT^2).

7. References

Alexander, R. M., 1949, "Fundamentals of Cyclone Design and Operation. Proceedings of Australian. Inst. Min. Metall. (New Series), pp152-153,203.

Boysan, F., Ayers, W. H. and Swithenbank, J., 1982, "A fundamental Mathematical Modelling Approach to Cyclone Design". Institution of Chemical Engineers, vol. 60, pp. 222-230.

Griffiths, W.D. and Boysan, F.,1996, "Computational Fluid Dynamics (CFD) and Empirical Modeling of Performance of a Number of Cyclone Sampers". Journal of Aerosol Science, vol. 27, n. 2, pp 281-304.

Hoekstra, a.j., derksen,J.J. and Van den Akker, H.E.A., 1999, "An Experimental and Numerical Study of Turbulent Swirling Flow in Gas Cyclones*"*. Chemical Engineering Science, vol. 54, pp. 2055-2065.

Leith, D., 1984,*"*Cyclones, Handbook of Powder Technology". Editors: Fayed, M.E. and Ottenm, L.; Van Nostrand Reinhold Company, New York, capítulo 16.

Meier, H.F., Mori, M., 1998; "Gas-Solid flow in Cyclones: The Eulerian-Eulerian approach". Computers Cemical Engineering, vol. 22, pp. S641-S644.

Ogawa, A., 1997, "Mechanical Separation Process and Flow Patterns of Cyclone Dust Collectors." Ind. Applied Mech. Ver , vol 50, n.3, pp. 97-130.

Ogawa, A., 1984, "Estimation of the Collection Efficiencies of the Three Types of the Cyclones Dust Collectors from the Standpoint of the Flow Patterns in the Cylindrical Cyclone Dust Collectors*"*. Bulletin of JSME, vol. 27, n.223, pp. 64-69.

Patankar, S.V., 1980, "Numerical Heat Transfer and Fluid Flow", Ed. Hemisphere Pub. Co., New York.

Patterson P.A and Munz, R.J.,1996,"Gas and Particle Flow Patterns at Room and Elevated Temperatures*"*. The Canadian Journal of Chemical Engineering, vol 74, April, pp. 213-221.

Peres, A.P., Kasper, F.R.S., Meier, H.F., Huziwara, W.K., Mori, M., 2001, "Análise de Modelos de Turbulência e da importância do refinamento da malha na simulação 3D do Escoamento gasoso em um ciclone." Anais do XVI Congresso Brasileiro de Engenharia Mecânica ,v.8, pp 79-87.

Peres, A. P., Meier, H.F.; Huziwara, W.K.; Mori, M., 2002, "Experimental Study and Advances in 3D Simulation of Gas Flow in Cyclone using CFD". European Symposium on Computer Aided Process Engineering, n. 12, pp. 943-948.

Shepherd, C.B. and Lapple, C.E., 1939, "Flow Pattern and Pressure Drop in Cyclone Dust Collectors". Ind. Engineering Chemical, vol 31, n. 8, pp. 972-983.

Shepherd, C.B. and Lapple, C.E., 1940. "Flow Pattern and Pressure Drop in Cyclone Dust Collectors: Cyclone Without Inlet Vane". Ind. Engineering Chemical, vol. 32, n. 9, pp. 1246-1252.

Slaterry, J.C., 1972, "Momentum, Energy and Mass Trasfer in Continua". Ed. McGraw- Hill Book Co., New York.

Ter Linden. A.J., 1949, "Investigations into Cyclone Dust Collectors". Proc. of the Institution of Mechanical Engineers. Vol 160, pp. 233-351.

Yuu, S., Jotaki, T.; Tomita, Y. and Yoshida, K., 1978, "The Reduction of Pressure Drop Due to Dust Loading in a Conventional Cyclone". Chem. Engineering Science, vol. 33, pp. 1573-1580.

8. Copyright Notice